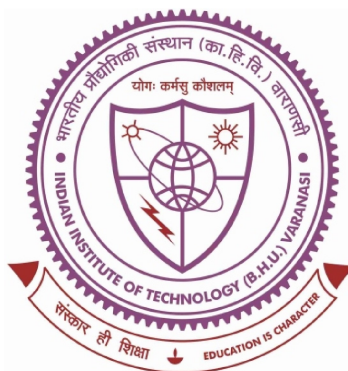


Synthesis and Electrochemical Performance of High Performing Pseudocapacitive Sulfide Electrodes for the Development of Supercapacitor/or Supercapattery



Thesis submitted in partial fulfillment for the
Award of Degree

Doctor of Philosophy

By

Vishal Kumar Kushwaha

DEPARTMENT OF CHEMISTRY
INDIAN INSTITUTE OF TECHNOLOGY
(BANARAS HINDU UNIVERSITY)
VARANASI- 221005
INDIA

Roll No. 17051504

Year 2023

*Dedicated to my Beloved Parents and
Family*



भारतीय
प्रौद्योगिकी
संस्थान
काशी हिन्दू विश्वविद्यालय

IIT

INDIAN
INSTITUTE OF
TECHNOLOGY
BANARAS HINDU UNIVERSITY

CERTIFICATE

It is certified that the work contained in the thesis titled "*Synthesis and Electrochemical Performance of High Performing Pseudocapacitive Sulfide Electrodes for the Development of Supercapacitor/or Supercapattery*" by "VISHAL KUMAR KUSHWAHA" has been carried out under my supervision and that this work has not been submitted elsewhere for a degree.

It is further certified that the student has fulfilled all the requirements of the comprehensive examination, candidacy and SOTA for the award of Ph.D. Degree.

Dr. Asha Gupta
(Supervisor)
Assistant Professor,
Department of Chemistry,
Indian Institute of Technology (BHU),
Varanasi - 221005, (U.P.), India

28/7/2023

Prof. K. D. Mandal
(Co-Supervisor)
Professor
Department of Chemistry,
Indian Institute of Technology (BHU),
Varanasi - 221005, (U.P.), India

28 July 2023

Head of the Department
Department of Chemistry,
Indian Institute of Technology (BHU),
Varanasi - 221005, (U.P.), India

विभागाध्यक्ष / HEAD

रसायन विज्ञान विभाग

Department of Chemistry

भारतीय प्रौद्योगिकी संस्थान (का.हि.वि.वि.)

Indian Institute of Technology (B.H.U.)

वाराणसी-२२१००५ / Varanasi - 221005



भारतीय
प्रौद्योगिकी
संस्थान
काशी हिन्दू विश्वविद्यालय

IIT INDIAN
INSTITUTE OF
TECHNOLOGY
BANARAS HINDU UNIVERSITY

DECLARATION BY THE CANDIDATE

I, **Vishal Kumar Kushwaha**, certify that the work embodied in this thesis is my own bonafide work carried out by me under the supervision of **Dr. Asha Gupta** from **Dec 2017 to July 2023**, at the **Department of Chemistry**, Indian Institute of Technology (BHU), Varanasi. The matter embodied in this thesis has not been submitted for the award of any other degree/diploma.

I declare that I have faithfully acknowledged and given credits to the research workers wherever their works have been cited in my work in this thesis. I further declare that I have not willfully copied any other's work, paragraphs, text, data, results, *etc.*, reported in journals, books, magazines, reports dissertations, thesis, *etc.*, or available on websites and have not included them in this thesis and have not cited as my own work.

Date:
Place: IIT (BHU), Varanasi

Signature of the student
(Vishal Kumar Kushwaha)

CERTIFICATE BY THE SUPERVISOR

It is certified that the above statement made by the student is correct to the best of my/our knowledge.

Dr. Asha Gupta
(Supervisor)
Department of Chemistry,
Indian Institute of Technology (BHU),
Varanasi - 221005, (U.P.), India

Prof. K. D. Mandal
(Co-supervisor)
Department of Chemistry,
Indian Institute of Technology (BHU),
Varanasi - 221005, (U.P.), India

Head of the Department 28 July 2023
Department of Chemistry,
Indian Institute of Technology (BHU),
Varanasi - 221005, (U.P.), India

विभागाध्यक्ष / HEAD
रसायन विज्ञान विभाग
Department of Chemistry
भारतीय प्रौद्योगिकी संस्थान (का.हि.वि.वि.)
Indian Institute of Technology (B.H.U.)
वाराणसी-२२१००५/Varanasi



भारतीय
प्रौद्योगिकी
संस्थान
काशी हिन्दू विश्वविद्यालय



INDIAN
INSTITUTE OF
TECHNOLOGY
BANARAS HINDU UNIVERSITY

COPYRIGHT TRANSFER CERTIFICATE

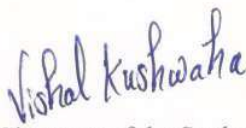
Title of the Thesis: *“Synthesis and Electrochemical Performance of High Performing Pseudocapacitive Sulfide Electrodes for the Development of Supercapacitor/or Supercapattery”*

Name of the Student: Vishal Kumar Kushwaha

Copyright Transfer

The undersigned hereby assigns to the Indian Institute of Technology (Banaras Hindu University) Varanasi all rights under copyright that may exist in and for the above thesis submitted for the award of the **“DOCTOR OF PHILOSOPHY”** degree.

Date: 28/07/2023
Place: IIT (BHU), Varanasi


Signature of the Student
(Vishal Kumar Kushwaha)

Note: However, the author may reproduce or authorize others to reproduce material extracted verbatim from the thesis or derivative of the thesis for the author's personal use provided that the source and the Institute's copyright notice are indicated.

Acknowledgments

The journey toward Ph.D. has been a turning point in my life, and it would not be possible without the constant support, assistance, and guidance that I have received from countless people. I would like to take this opportunity to acknowledge and appreciate those people who have given their valuable time during my Ph.D.

First of all, I would like to express my deep sense of gratitude to my supervisor **Dr. Asha Gupta**, Department of Chemistry, IIT(BHU), Varanasi, for her constant monitoring, enthusiastic encouragement, continued guidance, and unconditional support throughout my Ph.D. journey. I always admire her knowledge of the subject, her unconventional thinking, and her enthusiastic nature for research. Her ingenious approach to research is a source of inspiration, and this approach is reflected in her simple but clear writing style, which I want to carry forward in my career. I have been fortunate enough to be part of his group. Her suggestions and advice will always be beneficial in life, whether it is academic or nonacademic. I am very thankful to you ma'am for being a mentor academically as well as philosophically and wish to continue to seek this mentorship in future life too.

I would like to express my warmest gratitude to my co-supervisor **Prof. K. D. Mandal**, Department of Chemistry, IIT(BHU), Varanasi, for his valuable guidance, constant support, critical and motivating comments throughout the completion of this research work.

I would like to express my heartfelt thanks to **Dr. Preetam Singh**, Dept. of Ceramic engineering, IIT(BHU), Varanasi, for providing his valuable guidance, support, and encouragement throughout my research work.

My sincere thanks goes to my RPEC member **Dr. Indrajit Sinha** (Dept. of Chemistry, IIT-BHU), **Dr. Kundan Kumar** (Dept. of Ceramic engineering, IIT-BHU), and former RPEC member **Prof. Rajiv Prakash** (SMST, IIT-BHU), for providing valuable guidance.

I would like to express my gratitude to the Head, Department of Chemistry, IIT (BHU), Varanasi, Prof. Y. C. Sharma, and former HODs Prof. D. Tiwary and Prof. R. B. Rastogi for their kind support and for extending all required facilities to carry out my research work smoothly.

I am thankful to my seniors Dr. Rakesh Mandal, Dr. Neeraj Kumar Mishra, Dr. Vinod Kumar, Dr. Manish Kumar Verma, Dr. Akanksha Yadav for their suggestions and healthy discussions of my research issues. I am also thankful to my colleagues and juniors Mr. Abhay Narayan Singh, Mr. Neeraj Singh, Ms. Vaishali Soni, Ms. Shraddha Jaiswal, Mr. Krishna Gopal Nigam and Mr. Abijeet Singh for their support throughout my research work.

I would like to express my deepest affection to my parents, my brother and his wife, and my cute niece, for their love, concern, continuous moral support, and encouragement which enabled me to perform my liabilities. I also would like to thank my friends (Miss. Siddhi, Miss. Neha, Mr. Salman, and Mr. Shashikant) for their affection and support in my research work. I am thankful and indebted to MHRD for providing me financial support during my research work.

Date: 28/07/2023

Place: Varanasi



Vishal Kumar Kushwaha

(Research Scholar)

<u>Table of Contents</u>	Page No.
Acknowledgments.....	vi-vii
Table of Contents.....	viii-xiv
List of Figures	xv-xxiii
List of Tables.....	xxiv-xxv
List of Abbreviations	xxvi
Preface.....	xxvii-xxx

Chapter 1 Introduction and Literature Review

1.1 Global Energy Dependence and the Role of Renewables.....	1
1.2 Problems/Limitations with Renewable Energy Sources.....	3
1.3 Type of Renewable Energy Storage Solutions.....	4
1.3.1 Mechanical energy storage	4
1.3.2 Thermal energy storage.....	5
1.3.3 Superconducting Magnetic Energy Storage (SMES).....	6
1.3.4 Electrochemical energy storage devices	7
1.3.4.1 Types of Electrochemical Energy Storage Devices.....	8
1.3.4.2 Battery	9
1.3.4.2.1 Lead-acid battery.....	9
1.3.4.2.2 Lithium-ion battery.....	11
1.3.4.2.3 Redox Flow Battery.....	13
1.3.4.2.4 Metal-Air Battery	14
1.3.4.2.5 Metal-Sulphur Battery	15
1.3.4.3 Capacitors	17
1.3.4.4 Parameters of performances for grid-scale energy storage	20

1.3.4.5 Supercapacitors for grid-scale energy storage application	20
1.3.4.5.1 Pseudocapacitors	21
1.3.4.5.2 Classification of Pseudocapacitance	23
1.3.4.5.3 Hybrid supercapacitor	24
1.3.4.6 Electrochemical characteristics of different charge storage devices....	26
1.3.4.7 Factors affecting the performance of SCs	29
1.3.4.8 Electrode Materials for Supercapacitors Application	31
1.3.4.9 Pseudocapacitor Electrode Materials	32
1.3.4.9.1 Conducting polymers.....	32
1.3.4.9.2 Perovskite Oxides	33
1.3.4.9.3 Transition metal oxides	35
1.3.4.9.4 Transition metal sulfides.....	37
1.3.5 Nanomaterials and their scope in the context of energy storage.....	39
1.3.6 Suitability of Transition Metal Sulfides.....	40
1.3.7 Challenges and Methods of Synthesis in Transition Metal Sulfides.....	41
1.4 Scope of this work.....	42
1.5 References.....	43

Chapter 2 Synthesis and Characterization Techniques

2.1 Overview	61
2.2 Synthesis techniques.....	61
2.2.1 Solid-state method	63
2.2.2 Solution-based methods	64
2.3 Material Characterization Techniques.....	65
2.3.1 X-ray Diffraction (XRD).....	65

2.3.2 Scanning Electron Microscope (SEM)	67
2.3.3 Transmission Electron Microscopy (TEM)	68
2.3.4 Energy Dispersive X-Ray Spectroscopy (EDS)	70
2.3.5 BET (Brunner-Emmett-Teller theory) surface area measurement.....	71
2.3.6 TGA-DSC.....	72
2.3.7 UV-Visible Spectrophotometer.....	72
2.3.8 Fourier transform infrared (FTIR) spectroscopy.....	73
2.3.9 Raman Spectroscopy.....	74
2.3.10 X-ray Photoelectron Spectroscopy (XPS).....	74
2.3.11 Electrochemical Measurements.....	75
2.3.11.1 Cyclic voltammetry (CV).....	75
2.3.11.2 Galvanostatic Charge-Discharge (GCD).....	77
2.3.11.3 Electrochemical Impedance Spectroscopy (EIS)	77
2.4 Electrode Fabrication.....	78
2.5 Cell Assembly.....	79
2.6 References.....	81

Chapter - 3 - Nanocrystalline β -NiS: A Redox-Mediated Electrode in aqueous Electrolyte for Pseudocapacitor/Supercapacitor Applications

3.1 Introduction.....	85
3.2 Experimental:	86
3.2.1 Synthesis method	86
3.3 Results and Discussions:.....	87
3.3.1 XRD studies	87
3.3.2 Thermal analysis	88
3.3.3 Structural analysis.....	89

3.3.4 Bandgap measurement and surface area analysis	90
3.3.5 XPS analysis	91
3.3.6 FE-SEM and HR-TEM analysis	92
3.3.7 Electrochemical Studies:	94
3.3.7.1 Cyclic Voltammetry analysis	94
3.3.7.2 Determination of Diffusion Coefficient	96
3.3.7.3 Kinetics studies (determination of <i>b</i> values) and Dunn's plot analysis	97
3.3.7.4 Trassati's plot analysis.....	99
3.3.7.5 Chronoamperometry Charge/Discharge Analysis.....	100
3.3.7.6 Analysis of Electrochemical Impedance Spectroscopy (EIS)	102
3.3.7.7 Electrochemical charge storage behaviour in neutral Na ₂ SO ₄ electrolyte	103
3.3.7.8 Asymmetric full cell test of β-NiS//AC (CV, GCD, and cyclic stability)	105
3.3.7.9 Electrochemical Impedance Spectroscopy (EIS) of β-NiS//AC full cell	106
3.3.7.10 Study of energy density vs power density of β-NiS//AC full cell	107
3.4 Conclusions	108
3.5 References.....	111

Chapter - 4 - CoS Nano-Spheres: A Pseudocapacitive Electrode for Hybrid Supercapacitors

4.1 Introduction.....	117
4.2 Experimental :.....	118
4.2.1 Synthesis method.....	118
4.3 Results and Discussions:.....	119
4.3.1 XRD studies	119
4.3.2 Thermal analysis	120

4.3.3 Structural analysis.....	121
4.3.4 Bandgap measurement and surface area analysis	122
4.3.5 XPS analysis	123
4.3.6 FE-SEM and HR-TEM analysis	124
4.3.7 Electrochemical Studies:	126
4.3.7.1 Cyclic Voltammetry analysis	126
4.3.7.2 Determination of Diffusion Coefficient	129
4.3.7.3 Kinetics studies (determination of <i>b</i> values) and Dunn's plot analysis	130
4.3.7.4 Trassati's plot analysis.....	132
4.3.7.5 Chronoamperometry Charge/Discharge Analysis.....	133
4.3.7.6 Analysis of Electrochemical Impedance Spectroscopy (EIS)	135
4.3.7.7 Electrochemical charge storage behaviour in neutral Na ₂ SO ₄ electrolyte	136
4.3.7.8 Asymmetric full cell test of β-NiS//AC (CV, GCD, and cyclic stability)	138
4.3.7.9 Electrochemical Impedance Spectroscopy (EIS) of β-NiS//AC full cell	140
4.3.7.10 Study of energy density vs power density of β-NiS//AC full cell	141
4.4 Conclusions	143
4.5 References.....	144

Chapter - 5 - Ni_{0.5}Co_{0.5}S Nano-Chains: A High Performing Pseudocapacitive Electrode for Hybrid Supercapacitors

5.1 Introduction.....	151
5.2 Experimental:	152
5.2.1 Synthesis method.....	152

5.3 Results and Discussions:	153
5.3.1 XRD studies	153
5.3.2 Thermal analysis	154
5.3.3 Structural analysis.....	155
5.3.4 Bandgap measurement and surface area analysis	156
5.3.5 XPS analysis	157
5.3.6 FE-SEM and HR-TEM analysis	158
5.3.7 Electrochemical Studies:	159
5.3.7.1 Cyclic Voltammetry analysis	159
5.3.7.2 Determination of Diffusion Coefficient	162
5.3.7.3 Kinetics studies (determination of <i>b</i> values) and Dunn’s plot analysis	164
5.3.7.4 Trassati’s plot analysis.....	166
5.3.7.5 Chronoamperometry Charge/Discharge Analysis.....	167
5.3.7.6 Analysis of Electrochemical Impedance Spectroscopy (EIS)	169
5.3.7.7 Electrochemical charge storage behaviour in neutral Na ₂ SO ₄ electrolyte	170
5.3.7.8 Asymmetric full cell test of β-NiS//AC (CV, GCD, and cyclic stability)	172
5.3.7.9 Electrochemical Impedance Spectroscopy (EIS) of β-NiS//AC full cell	174
5.3.7.10 Study of energy density vs power density of β-NiS//AC full cell	174
5.4 Conclusions	176
5.5 References	178
 Chapter - 6 - SrFeO_{3-δ}: A Novel Fe⁴⁺↔Fe²⁺ Redox Mediated Pseudocapacitive Electrode in Aqueous Electrolyte	
6.1 Introduction	185

6.2 Experimental:	187
6.2.1 Synthesis method	187
6.3 Results and Discussions:	187
6.3.1 XRD studies	187
6.3.2 XPS analysis	189
6.3.3 BET-surface area analysis	190
6.3.4 Structure, FE-SEM and HR-TEM analysis	191
6.3.5 Electrochemical Studies:	193
6.3.5.1 Cyclic Voltammetry analysis	193
6.3.5.2 Kinetics Studies and Trassati's Plot Analysis	195
6.3.5.3 Determination of Diffusion Coefficient and Dunn's Plot Analysis	197
6.3.5.4 Charge/Discharge analysis and cyclic stability test	200
6.3.5.5 Analysis of Electrochemical Impedance Spectroscopy (EIS)	201
6.3.5.6 Structural stability test	202
6.3.5.7 Asymmetric Full Cell Test of SrFeO_{3-δ}//AC (CV, GCD and Cyclic Stability)	203
6.3.5.8 Electrochemical Impedance Spectroscopy (EIS) of SrFeO_{3-δ}//AC Full Cell	205
6.4 Conclusions	207
6.5 References	210

Chapter - 7 - Summary and Future scope

7.1 Summary	217
7.2 Future Scope	222

Figure No.	Figure description	Page No.
Figure 1.1	Global energy usage in 2013 as a percentage of energy sources	1
Figure 1.2	Renewable energy sources	3
Figure 1.3	Structure of a Flywheel with components	5
Figure 1.4	Schematic of the sensible heat storage system	6
Figure 1.5	Block diagram of a SMES system	7
Figure 1.6	Classification of rechargeable Electrochemical Energy storage systems	8
Figure 1.7	Scheme of prismatic and spiral wound construction of Lead Acid battery	11
Figure 1.8	Schematic diagram of Li-ion battery	12
Figure 1.9	Construction of prismatic and cylindrical Li-ion cell construction	13
Figure 1.10	Schematic mechanism of a Redox Flow Battery	14
Figure 1.11	Schematic diagrams of Li-air battery	15
Figure 1.12	Li-S cell schematic showing its charge and discharge processes	17
Figure 1.13	Schematic illustration of a conventional capacitor	18
Figure 1.14	Charge storage schematics in (a) dielectric and (b) electrolytic capacitor are shown in the diagram	19
Figure 1.15	Schematic diagram about charge-storage mechanisms of various pseudocapacitive materials: (a) underpotential deposition, (b) redox pseudocapacitor and (c) ion intercalation pseudocapacitor.	24
Figure 1.16	Hybrid supercapacitor	25

Figure 1.17	Shows typical cyclic voltammograms (CV) and galvanostatic discharging curves for different types of electrochemical energy-storage materials	27
Figure 1.18	Components responsible for tuning the performance of the SCs	31
Figure 2.1	Characterization techniques used	65
Figure 2.2	Schematic diagram of the incident and diffracted X-rays from the crystal lattice	66
Figure 2.3	Schematic diagram of SEM operating	68
Figure 2.4	Schematic diagram of TEM showing interaction of electrons with sample	70
Figure 2.5	Schematic diagram of UV-Visible spectrometer	73
Figure 2.6	Three electrodes setup used in electrochemical measurement	76
Figure 2.7	Typical Nyquist plot for electrode	78
Figure 2.8	Assembled electrode picture for electrochemical measurement	79
Figure 3.1	(a) Rietveld refinement of the XRD profile of β -NiS nanoparticles and (b) VESTA image of β -NiS nanoparticles	87
Figure 3.2	(a) TGA of β -NiS nanoparticles in an N ₂ atmosphere (inset shows the DTA plot)	89
	(b) FT-IR spectra of β -NiS nanoparticles and (c) Raman spectra of β -NiS nanoparticles	90
	(d) UV-Visible spectra of β -NiS nanoparticles (inset shows Tauc plot for the β -NiS) and (e) BET nitrogen adsorption/desorption isotherm of β -NiS nanoparticles	91
Figure 3.3	XPS plot of β -NiS nanoparticles, (a) Ni (2p) spectra and (b) S (2p) spectra	91
Figure 3.4	(a) FE-SEM images, (b) EDX analysis image of the prepared β -NiS nanoparticles, (c) HRTEM images of β -NiS nanoparticles, (d)	93

	SAED pattern shows the lattice, (e) lattice fringes β -NiS nanoparticles. Inset (i, ii, and iii) of (e) show FFT image, inverse FFT, and d-spacing β -NiS nanoparticles	
Figure 3.5	(a) shows the plot of KOH concentrations vs. specific capacitance at various scan rates. Typical CV curves for β -NiS electrode in (b) 1 M, (c) 2 M and (d) 4 M KOH solutions at different scan rates of 1, 5, 10, 60 and 100 mVs^{-1} , and (e) shows the comparative CV study in different concentrations of electrolytes at 10 mV/s	95
	(f) shows plot of peak current vs. square root of the scan rate for diffusion kinetics of β -NiS electrode	97
Figure 3.6	Electrodynamic characteristics of the β -NiS electrode; (a) plot of the linear relationship between $\log(\text{peak current})$ and $\log(\text{scan rate})$ at two different scan rate regions, (b) plot of the power law of the charged state at potential and discharged state at a potential, (c) diffusive and capacitive contribution at different scan rates, and (d) analysis of kinetic contribution at 10 mVs^{-1}	98
	(e, f) Trasatti plot at different scan rates	100
Figure 3.7	(a) Charge/discharge curve of β -NiS electrode, (b) capacitance performance of β -NiS electrode at different constant current density, (c) capacitance retention and coulombic efficiency β -NiS electrode, and (d) shows the comparative study of GCD at 1 M, 2 M and 4 M KOH concentration	101
	(e) Nyquist and (f) Bode plot of β -NiS electrode at 10 mV between 0.1 and 100 kHz (inset displays enlarged view of Nyquist plot at high-frequency region)	102
Figure 3.8	(a) CV and (b) GCD plot of β -NiS electrode in 0.5 M Na_2SO_4 electrolyte, (c) Comparative CV diagram of β -NiS electrode in 2 M KOH and 0.5 M Na_2SO_4 electrolyte at 10 mV/s and (d) Comparative charge/discharge curve of β -NiS electrode in KOH and Na_2SO_4 medium at 1A/g	104

Figure 3.9	<p>(a) Separate CV plots for activated carbon and β-NiS electrode in 2 M KOH Electrolyte 10 mV/s, (b) CV at different scan rates, (c) charge-discharge at different current rates and (d) Capacitance retention and coulombic efficiency</p> <p>(e) Nyquist and (f) Bode plot at 10 mV at initial cycle and after 2500 cycle of full cell formation</p> <p>(g) Ragone plot of the β-NiS//AC fuel cell in ASC mode in comparison with reported supercapacitor devices</p>	<p>106</p> <p>107</p> <p>108</p>
Figure 4.1	<p>(a) Rietveld refined XRD profile of CoS nano-sphere, (b) and (c) VESTA image of CoS nano-sphere</p>	<p>119</p>
Figure 4.2	<p>(a) TGA of CoS nano-sphere in an N₂ atmosphere (inset shows the DTA plot)</p> <p>(b) FT-IR spectra and (c) Raman spectra of CoS nano-sphere</p> <p>(d) UV-Visible spectra (inset shows Tauc plot) and (e) BET surface area plot using nitrogen adsorption/desorption isotherm of CoS nano-sphere</p>	<p>121</p> <p>121</p> <p>123</p>
Figure 4.3	<p>Deconvoluted XPS plot of CoS nano-sphere, (a) Co (2p) spectra, and (b) S (2p) spectra</p>	<p>123</p>
Figure 4.4	<p>(a) FE-SEM (b) EDX image of the prepared CoS nano-sphere, (c) HRTEM images of CoS nano-sphere, (d) SAED pattern shows diffused ring pattern for lattice plane diffractions, (e) lattice fringes representing [100] plane of CoS nano-sphere. The inset of (e) shows FFT, inverse FFT image</p>	<p>125</p>
Figure 4.5	<p>(a) shows the plot of KOH concentrations vs. specific capacitance at different scan rates. Typical CV curves for CoS electrode in (b) 0.5, (c) 1, (d) 2 and (e) 4 M KOH solutions at different scan rates of 1-100 mVs⁻¹. (f) shows the comparative CV study in different concentrations of electrolytes at 10 mV/S</p>	<p>127</p>

	(g) shows plot of peak current vs. square root of the scan rate for diffusion kinetics for the CoS electrode	129
Figure 4.6	Electrochemical kinetics of the CoS electrode (a) plot of between log (peak current) vs. log (scan rate) at two different scan rate regions, (b) plot of the power law at charged state and discharged state, (c) diffusive and capacitive contribution of the electrode at different scan rates and (d) capacitance contribution at 10 mVs ⁻¹ (e, f) Corresponding to Trasatti plot at different scan rates	131 132
Figure 4.7	(a) Galvanostatic charge/discharge (GCD) curve of the CoS electrode, (b) capacitance performance of the CoS electrode at various current densities, (c) capacitance retention and coulombic efficiency of the CoS electrode and (d) comparative study of GCD at different electrolyte concentration (e) fitted Nyquist plot, (f) comparative Nyquist plot before and after long term cyclic stability and (g) Bode plot at 10 mV between 100 kHz - 0.1 Hz	134 135
Figure 4.8	(a) CV and (b) GCD plot in 0.5 M Na ₂ SO ₄ electrolyte, (c) Comparative CV plot in 2 M KOH and 0.5 M Na ₂ SO ₄ electrolyte at the scan rate of 10 mV/s and (d) Comparative charge/discharge plot in 2 M KOH and 0.5 M Na ₂ SO ₄ electrolyte at the current density of 1 A/g of the CoS electrode	137
Figure 4.9	(a) Separate CV plots for AC and CoS electrode in 2 M KOH Electrolyte 10 mV/s, (b) CV and (c) GDC of the full cell in HSC mode at different current rates and (d) Capacitance retention and coulombic efficiency (e) Nyquist and (f) Bode plot at 10 mV at initial cycle and after 10000 cycle of full cell formation (g) Ragone plot of the CoS//AC full cell in HSC mode in comparison with reported supercapacitor devices	139 140 142

Figure 5.1	Schematic illustration of the synthesis of Ni _{0.5} Co _{0.5} S	153
Figure 5.2	(a) Shows Rietveld refinement of the XRD profile and (b) VESTA image of Ni _{0.5} Co _{0.5} S nano-chains	154
Figure 5.3	(a) TGA of Ni _{0.5} Co _{0.5} S nano-chains in an N ₂ atmosphere	155
	(b) FT-IR spectra and (c) Raman spectra of Ni _{0.5} Co _{0.5} S nano-chains	156
	(d) UV-Visible spectra (inset shows Tauc plot) and (e) BET nitrogen adsorption/desorption isotherm of Ni _{0.5} Co _{0.5} S nano-chains	157
Figure 5.4	XPS plot of Ni _{0.5} Co _{0.5} S nano-chains, (a) Ni (2p) spectra, (b) Co (2p) spectra, and (c) S (2p) spectra	158
Figure 5.5	(a) SEM image, (b) EDX analysis (c & d) HRTEM images of Ni _{0.5} Co _{0.5} S nano-chains	159
Figure 5.6	(a) Illustrates the plot of KOH concentrations vs. specific capacitance at different scan rates. Typical CV curves for Ni _{0.5} Co _{0.5} S electrode in (b) 1, (c) 2, and (d) 4 M KOH solutions at different scan rates of 1-100 mVs ⁻¹ , and (e) shows the comparative CV study in different concentrations of electrolytes at 10 mVs ⁻¹	161
	(f) Plot of peak current vs. square root of the scan rate for diffusion kinetics of Ni _{0.5} Co _{0.5} S electrode	163
Figure 5.7	Electrodynamic characteristics of the Ni _{0.5} Co _{0.5} S electrode; (a) plot of the linear relationship between log (peak current) and log (scan rate) at two different scan rate regions, (b) plot of the power law of the charged state at potential and discharged state at a potential, (c) diffusive and capacitive contribution at different scan rates, and (d) analysis of kinetic contribution at 10 mVs ⁻¹	165
	(e, f) Trasatti plot at different scan rates for Ni _{0.5} Co _{0.5} S electrode	167
Figure 5.8	(a) Charge/discharge curve of Ni _{0.5} Co _{0.5} S electrode, (b) capacitance performance of Ni _{0.5} Co _{0.5} S electrode at different constant current density, (c) capacitance retention and coulombic efficiency	168

	Ni _{0.5} Co _{0.5} S electrode, and (d) shows the comparative study of GCD at 1, 2, and 4 M KOH concentration	
	(e) Nyquist and (f) Bode plot of Ni _{0.5} Co _{0.5} S electrode at 10 mV between 0.1 Hz and 100 kHz (inset displays enlarged view of nyquist plot at high-frequency region)	170
Figure 5.9	(a) CV and (b) GCD plot of Ni _{0.5} Co _{0.5} S electrode in 0.5 M Na ₂ SO ₄ electrolyte, (c) Comparative CV diagram of Ni _{0.5} Co _{0.5} S electrode in 4 M KOH and 0.5 M Na ₂ SO ₄ electrolyte at 10 mVs ⁻¹ , and (d) Comparative charge/discharge curve of Ni _{0.5} Co _{0.5} S electrode in KOH and Na ₂ SO ₄ medium at 1 A/g	171
Figure 5.10	(a) Separate CV plots for activated carbon and Ni _{0.5} Co _{0.5} S electrode in 4 M KOH Electrolyte 10 mV/s, (b) CV at different scan rates, (c) charge-discharge at different current rates, and (d) Capacitance retention and coulombic efficiency	173
	(e) Nyquist and (f) Bode plot at 10 mV at initial cycle and after 10000 cycles of full cell formation	174
	(g) Ragone plot of the Ni _{0.5} Co _{0.5} S//AC full cell in ASC mode in comparison with reported supercapacitor devices	175
Figure 6. 1	(a) Rietveld refined powder-XRD pattern and (b) Vesta image of SrFeO _{3-δ}	188
	The core-level XPS of (c) Fe2 <i>p</i> , (d) Sr3 <i>d</i> and (e) O1 <i>s</i> spectrum	189
	(f) BET surface area N ₂ adsorption-desorption isotherms with pore-size distribution	190
Figure 6. 2	(a) Supercell (2x2x2) structure of stoichiometric-SrFeO ₃ in cubic-perovskite structure, (b) (110) plane containing Sr ²⁺ , Fe ⁴⁺ and O ²⁻ ions, (c) (111) plane containing only Fe ⁴⁺ ions. Blue, green and red balls correspond to Sr, Fe and O ions	191
	(d) SEM images of as-prepared SrFeO _{3-δ} , (e, f) HRTEM images of as-prepared SrFeO _{3-δ} showing lattice fringes with <i>d</i> -spacing	192

corresponding to (110) plane before and after the complete discharge cycle and **(g)** selected area electron diffraction (SAED) pattern of the sample after complete discharge cycle

- Figure 6.3** **(a)** SEM image of the area of interest, **(b)** Sr map, **(c)** Fe map, **(d)** Elemental analysis showing Fe: Sr ratio the as-prepared powder sample of $\text{SrFeO}_{3-\delta}$ 192
- Figure 6.4** **(a)** KOH concentrations vs specific capacitance at different scan rates. Typical CV curves for $\text{SrFeO}_{3-\delta}$ in **(b)** 0.1 M, **(c)** 1 M, **(d)** 2 M @ 1mV/s, **(e)** 2 M and **(f)** 6 M KOH solution at different scan rates of 1, 10, 50 and 100 mV/s 194
- Figure 6.5.** **(a, b)** Plot showing the total capacitance C_{Total} and amount of charge stored at the outer surface C_{dl} estimated by the Trassati plot 197
- (c)** The slope of $\log_{10} I(V)$ vs. $\log_{10} v$ shows b value at the cathodic (-0.8 V) and anodic peak potential (-0.7 V), **(d)** b value plot at various potentials, **(e)** K_1 and K_2 values are obtained from Dunn's method, **(f)** Plot showing the capacitive contribution (white shaded area) and diffusion-controlled process (red-pink line shaded area) at a scan rate of 10 mV s⁻¹, and **(g)** Capacitive contributions at different scan rate 199
- Figure 6.6** **(a)** Galvanostatic charge/discharge curves measured with different current densities in 2 M KOH, **(b)** Cycle number versus capacitance from GCD at different current densities and **(c)** capacitance retention and coulombic efficiency plot of $\text{SrFeO}_{3-\delta}$. 201
- (d)** Impedance spectra measured at 0 and -0.4V in a three-electrode configuration in 2 M KOH; inset compares the impedance spectra obtained after cycle 1 and 2500 of repeated charge discharge scans 202
- Figure 6.7** **(a)** Separate CV plots for activated carbon and $\text{SrFeO}_{3-\delta}$ electrode in 2 M KOH Electrolyte 10 mV/s, **(b)** CV at different scan rates, **(c)** Charge-discharge at different current rates, and **(d)** Capacitance retention and coulombic efficiency 204

(e) Nyquist at 10 mV at initial cycle and after 5000 cycles of full cell formation	205
(f) Ragone plot of the $\text{SrFeO}_{3-\delta}$ //AC full cell in ASC mode in comparison with reported supercapacitor devices	206

TABLES

Table No.		Page No.
Table 1.1	Comparisons between batteries, capacitor, and supercapacitor	29
Table 1.2	Literature review on several perovskite oxide-based supercapacitors and their specific values	35
Table 1.3	Literature review on several metal oxide-based supercapacitors and their specific values	37
Table 1.4	Literature reviews of TMS based supercapacitors and its specific capacitance	38
Table 3.1	X-ray crystallographic representative diffraction data for β -NiS nanoparticles	88
Table 3.2	Displays the Ragone plot of β -NiS electrode//AC (ASC) device in comparison with reported supercapacitor devices.	108
Table 3.3	Values of specific capacitance of some transition-metal sulfides	110
Table 4.1	Ionic properties of the aqueous electrolytes	137
Table 4.2	The performances of the CoS//AC full cell in HSC mode compared with other reported full cell supercapacitors	142
Table 5.1	Displays the Ragone plot of the $\text{Ni}_{0.5}\text{Co}_{0.5}\text{S}$ electrode//AC (ASC) full cell compared with reported supercapacitor devices	176
Table 6.1	Binding energies (in eV) for XPS core-level main peaks	190
Table 6.2	Displays the Ragone plot of the $\text{SrFeO}_{3-\delta}$ //AC (ASC) full cell compared with reported supercapacitor devices	207
Table 6.3	Values of specific capacitance of some transition-metal oxides. Nano-structured materials and carbon/graphene-modified oxide	208

materials are excluded from the list for the likeness of comparison of common transition-metal oxides with $\text{SrFeO}_{3-\delta}$.

Table 7.1	Displays the comparative study of BET-specific surface area and capacitance of the different electrode materials used	221
Table 7.2	Table 7.2 Displays the electrochemical characteristics of the fabricated ASC full cells	222

LIST OF ABBREVIATIONS

XRD- X-ray Diffraction

HR-SEM-High-Resolution Scanning Electron Microscope

HR-TEM-High-Resolution Transmission Electron Microscope

TGA- Thermogravimetric Analysis

FTIR -Fourier Transform Infrared Spectroscopy

XPS-X-ray Photoelectron Spectroscopy

BET - (Brunauer, Emmett, and Teller) specific surface

CV- Cyclic Voltammetry

ASCs - Asymmetric Supercapacitors

Csp - Specific Capacitance

HSCs – Hybrid Supercapacitors

Preface

The development of high-performance efficient energy storage systems devices propelled immense research interest to provide a sustainable energy supply to the world by utilizing the full potential of renewable energy sources. Traditional solutions like lithium-ion batteries suffer from high costs, poor performance at high current rates, and environmental impact restrictions. Pseudocapacitive materials, with their high specific capacitance and rapid charge/discharge rates, have emerged as promising candidates for overcoming the limitations of conventional supercapacitors and batteries. Transition metal sulfides (TMS) have garnered significant attention due to their abundance, low cost, efficient energy storage ability, and remarkable electrochemical properties compared to other electrodes.

This thesis entitled “*Synthesis and electrochemical performance of high performing pseudocapacitive sulfide electrodes for the development of supercapacitor/or supercapattery*” explores the potential of TMS as pseudocapacitive materials for efficient energy storage electrodes. The study's primary goals are to understand the fundamental electrochemical processes, elucidate the charge storage mechanisms, and optimize the transition metal sulfide electrode performance. The thesis explores the kinetics and thermodynamics of the electrochemical charge storage processes occurring at TMS-based electrodes. This involves the study of charge transfer kinetics, surface redox reactions, ion diffusion, and the influence of electrolytes on the overall performance. The following chapters comprise the structure of this current thesis:

The **first chapter** begins with a brief overview of energy sources and explores alternative energy sources of fossil fuels, including renewable and non-renewable. This chapter mainly discusses electrochemical energy storage (EES) systems categorizing

them based on their charge storage mechanism and compiling various phenomena associated with capacitors, batteries and pseudocapacitors. The main section of this chapter concludes by highlighting the significant output of this research, which is the identification of redox-mediated intercalative pseudocapacitive electrodes.

The **second chapter** provides a concise overview of the experimental methodology, encompassing the synthesis techniques for producing materials with controlled morphology and composition and their characterizations along with electrochemical techniques to measure the electrode's performances and to analyze charge storage mechanism.

In the **third chapter**, I discuss in detail about synthesis, characterizations, and electrochemical performances of nanocrystalline β -NiS. The electrode shows the excellent specific capacitance of 1578 F/g at 1 A/g from the galvanostatic discharge profile in 2M KOH aqueous electrolyte due to the reversible transformation of Ni^{2+} to Ni^{3+} through electrosorption (redox) of OH^- ions. Further, the b -value from the power law for charge storage kinetics/mechanisms attributed to semi-infinite diffusion-controlled and surface-control redox (non-diffusion) mediated pseudocapacitance processes responsible for the high specific capacitance of β -NiS nanoparticles.

The **fourth chapter** of the thesis describes the synthesis and characterization of hexagonal CoS nano-spheres, and put detailed discussion about the structural and electrochemical properties of layered CoS nano-spheres. The CoS electrode displayed an excellent specific capacitance of 761 F/g at 1 A/g current density due to the reversible transformation of $\text{Co}^{2+} \rightleftharpoons \text{Co}^{3+}$ through electrosorption (redox) of OH^- ions coupled with EDLC-type surface contribution of capacitance in 2 M KOH aqueous electrolyte. An aqueous asymmetric hybrid supercapacitor (HSC) device was fabricated using CoS as the positive electrode and the activated carbon (AC) as the negative

electrode. The asymmetric HSC device results in high energy and power densities of 139.7 Wh/kg and 7.51 kW/kg, respectively, which shows excellent cyclic stability of up to 87% after 10000 continuous charge-discharge cycles.

In the **fifth chapter**, nano-chains architectures of $\text{Ni}_{0.5}\text{Co}_{0.5}\text{S}$ electrode materials consisting of interconnected nano-spheres are rationally designed by tailoring the surface structure to develop high-performance supercapacitive electrodes. Nano-chains of bimetallic sulfide $\text{Ni}_{0.5}\text{Co}_{0.5}\text{S}$ electrode exhibited a highly improved electrochemical performance achieving the specific capacity of 2190 F/g at 1 A/g in 4 M KOH aqueous electrolyte. Furthermore, an impressive energy density equivalent to ~ 257 Wh/kg and power density of ~ 7.2 kW/kg was achieved by the assembled $\text{Ni}_{0.5}\text{Co}_{0.5}\text{S}/\text{AC}$ two electrode full cell in ASCs mode where AC acted as the negative electrode and the $\text{Ni}_{0.5}\text{Co}_{0.5}\text{S}$ electrode as the positive electrode in 4 M KOH electrolyte.

In the **sixth chapter**, I present the detailed study of perovskite type $\text{SrFeO}_{3-\delta}$ prepared by flux-method which shows superior pseudo-capacitive charge storage as the negative electrode of a pseudo-capacitor or supercapacitor with superior stability. $\text{SrFeO}_{3-\delta}$ offers high specific capacitances of 743 F/g at a current density of 1 A/g due to the participation of $\text{Fe}^{4+/3+}$ and $\text{Fe}^{3+/2+}$ redox couples. Further $\text{SrFeO}_{3-\delta}$ demonstrates excellent cyclic stability which is attributed to the inherent metallic electrical conductivity of $\text{SrFeO}_{3-\delta}$ and the fortuitous tendency of the robust cation framework structure to accommodate flexible oxygen content.

The concluding **seventh chapter** presents an overview of nano-structured transition metal sulfides (TMS) as a novel pseudocapacitive electrode for adequate electrochemical energy storage. Superior performances of the electrodes were obtained due to active participation and the reversible transformation of $\text{M}^{2+/3+}$ redox couple through electrosorption (redox) of OH^- ions coupled with EDLC-type surface

contribution of capacitance. Further metallic SrFeO_{3-δ} is presented as a robust negative pseudocapacitive electrode as an alternative to AC. Redox mediated interconversion $O^{2-} + H_2O \rightleftharpoons 2OH^-$ was found as the key component behind superior pseudocapacitive charge storage in the perovskite SrFeO_{3-δ} electrode.